

MEF2D/Wnt/ β -catenin pathway regulates the proliferation of gastric cancer cells and is regulated by microRNA-19

Kai Xu¹ · Ying-chao Zhao²

Received: 9 November 2015 / Accepted: 29 December 2015 / Published online: 13 January 2016
© International Society of Oncology and BioMarkers (ISOBM) 2016

Abstract The underlying molecular pathogenesis in gastric cancer remains poorly unknown. The transcription factor myocyte enhancer factor 2D (MEF2D) participates in the initiation and development of many human cancers. However, its potential roles in gastric cancer have surprisingly not been studied. In present study, we first explored MEF2's expression in gastric cancer, finding that only MEF2D rather than MEF2A, 2B, or 2C was elevated in gastric cancer clinical specimens. Furthermore, immunohistochemical analysis on the tissue samples obtained from 260 patients with gastric cancer revealed that MEF2D expression was significantly associated with the clinical stage, vascular invasion, metastasis, and tumor size. Gastric cancer patients with MEF2D expression showed a significantly shorter overall survival time compared with that of patients lacking of MEF2D. Multivariate analysis revealed that MEF2D expression was an independent prognostic factor for overall survival. These results indicated that MEF2D was a prognostic marker for gastric cancer. Notably, MEF2D silencing was able to reduce the proliferation and survival of gastric cancer cells. Further study revealed that MEF2D suppression significantly inactivated the oncogenic Wnt/ β -catenin pathway. Downregulation of MEF2D inhibited the tumorigenesis of gastric cancer cells in nude mice. Finally, MEF2D is a direct target of miR-19, which

was found to be decreased in gastric cancer clinical specimens. Collectively, we found that miR-19/MEF2D/Wnt/ β -catenin regulatory network contributes to the growth of gastric cancer, hinting a new promising target for gastric cancer treatment.

Keywords Gastric cancer · MEF2D · MicroRNA-19 · Wnt · β -catenin

Introduction

Gastric cancer (GC) is a highly lethal cancer, with increasing incidence worldwide [1]. Poor understanding on molecular mechanisms underlying tumorigenesis of GC leads to lack of effective treatment [2]. Intensive studies focus on identification of GC-related genes [3–5]. Many transcription factors, such as caudal-related homeobox family genes, have been demonstrated to participate in GC tumorigenesis and progression [6–8]. However, molecular pathogenesis of GC is not fully understood. Thus, it is necessary to identify novel molecular targets involved in GC tumorigenesis.

Myocyte enhancer factor 2D (MEF2D) is a transcription factor belonging to MEF2 family (MEF2A, 2B, 2C, and 2D) [9]. They were initially identified as major transcription activators in muscle development [10]. Recently, MEF2 family members were shown to participate in the initiation and progression of human cancers. MEF2C and MEF2D are involved in the progression of hepatocellular carcinoma via VEGF signaling pathway [11–13]. In addition, MEF2s are shown to play vital roles in initiation and metastasis of hepatocellular carcinoma [14]. Further study identifies *MEF2D* gene as a potential oncogene in the development of leukemia [15, 16]. Also, recent studies demonstrate that MEF2D is closely related with lung carcinoma [17, 18]. However, experimental

✉ Ying-chao Zhao
zhaoyingchao999@163.com

¹ Department of Otolaryngology-Head and Neck Surgery, Tongji Hospital, Tongji Medical College, Huazhong University of Science and Technology, Wuhan, China

² Department of Cancer Center, Union Hospital, Tongji Medical College, Huazhong University of Science and Technology, Wuhan 430022, China

evidence about the role of MEF2D in GC tumorigenesis is still lacking so far.

In this study, we first investigated MEF2D expression and function in gastric cancer. Further, we studied the potential downstream pathway involved in the effect of MEF2D in gastric cancer. Finally, we explored the possible regulatory mechanism of MEF2D upregulation in gastric cancer.

Materials and methods

Cell culture and animal preparation

AGS and MKN28 gastric cell lines were purchased from Chinese Academy of Sciences and cultured in the Dulbecco's modified Eagle medium (DMEM) (Invitrogen-Life Technologies, Carlsbad, CA, USA) supplemented with 10 % fetal bovine serum (Invitrogen-Life Technologies, Carlsbad, CA, USA) containing penicillin/streptomycin. The cells were grown in a humidified 5 % CO₂ at 37 °C in an incubator.

BALB/c female nude mice, 6-week-old, were bought from the Experimental Animal Center of Tongji Medical College, Huazhong University of Science and Technology (Wuhan, China) and housed under pathogen-free conditions with free access to water and food. The animal experimental procedures were approved and reviewed by the Institutional Animal Care and Use Committee of Tongji Medical College, Huazhong University of Science and Technology.

Gastric cancer specimen collection

In total, 30 fresh samples of gastric cancer and paired adjacent normal gastric tissues were collected from gastric cancer patients from April 1, 2015 to December 1, 2015 at Tongji Hospital and used for reverse transcriptase quantitative PCR (RT-qPCR) and western blot to determine the MEF2's expression levels. In addition, tissue samples collected from 260 patients that underwent surgery for the treatment of gastric cancer between January 1, 2005 and December 30, 2010 at Tongji Hospital were used for immunohistochemical analysis. The group included 160 males and 100 females, with a mean age of 63.2 ± 13.4 years. The present study was performed with all patients' written informed consent and in accordance to the procedures approved by Ethical Review Board in Tongji Medical College.

Follow up

All tissue samples were used for immunohistochemical analysis. All patients underwent gastrectomy and were monitored by chest, abdominal, and pelvic computed tomography (CT) and blood testing at 3-month intervals and yearly gastroscopy.

The overall survival time was defined as the time between surgery and clinically or radiologically confirmed recurrence or metastasis, or mortality.

Real-time quantitative PCR

Total RNAs were extracted from the tissues as well as the cell lines with TRIzol reagent (FBS, Invitrogen, Carlsbad, CA), according to the instructions of the manufacturer. Reverse transcription was performed with the QuantiMir RT kit (System Biosciences). Primers for MEF2D: forward, 5'-AGGGAAATAACCAAAAACTACCAAA-3', reverse, 5'-GCTACATGAACACAAAAACAGAGACC-3'; primers for miR-19: forward, 5'-TGATAATTAGCAAGCAGGATTA-3', reverse, 5'-ACCAACATTACGCGGCATCATT-3'; primers for glyceraldehyde-3-phosphate dehydrogenase (GAPDH): forward, 5'-GCGAGATCGCACTCATCT-3', reverse, 5'-TCAGTGGTGGACCTGACC-3'. Primers for control U6: forward, 5'-CTCGCT TCGGCAGCACA-3', reverse, 5'-AACGCTTACGAATT TGCCT-3'.

MEF2D was amplified as follows: denaturation at 95 °C for 10 min and then 40 cycles of 95 °C for 15 s and 60 °C for 1 min. miR-19 was amplified as follows: denaturation at 95 °C for 10 min and then 40 cycles of 95 °C for 10 s, 60 °C for 20 s, and 72 °C for 10 s. U6 RNA was used as an microRNA (miRNA) internal control, and GAPDH was used to normalize the amount of total messenger RNA (mRNA) in each sample. All values were calculated as ratios normalized to U6 or GAPDH.

Immunohistochemistry

Immunohistochemistry staining was performed on the collected clinical gastric cancer sections to detect the expression of MEF2D. Briefly, formalin and paraffin were used to fix and embed the tissues, respectively. The samples were heated to retrieve the antigen. Antibodies recognizing MEF2D (Sigma-Aldrich, MO, USA) were employed to stain the protein, followed by counterstaining of nuclei with hematoxylin. The levels of MEF2D were semi-quantitatively based on the intensity and percentage of staining. The MEF2D staining was classified as strong (3+), moderate (2+), weak (1+), or absent (–) compared with the adjacent non-cancerous tissues. Scores of 0 or 1+ were considered to indicate a lack of MEF2D expression, and scores of 2+ or 3+ were considered to indicate the presence of MEF2D expression.

The detection of proliferation rates

AGS and MKN28 gastric cancer cells (4×10^3), which are pretreated with scramble lentivirus (Lv-scramble) or Lv-shMEF2D (multiplicity of infection (MOI)=10) (Shanghai Genepharma Co. Ltd., Shanghai, China), respectively, were

seeded in each well of 96-well plates. At the indicated time points, the number of cells in each well was determined with Scepter Handheld Automated Cell Counter (Millipore, MA).

Terminal deoxynucleotidyl transferase (TdT) dUTP nick-end labeling assay

Apoptotic cells were detected using a terminal deoxynucleotidyl transferase (TdT) dUTP nick-end labeling (TUNEL) kit (Sigma, St. Louis, MO, USA) according to the manufacturer's instructions. Briefly, cells were cultured on cover slips for 48 h. Then, the cells were fixed in 4 % paraformaldehyde solution in phosphate-buffered saline (PBS) for 30 min at room temperature. The cells were then incubated with a methanol solution containing 0.3 % H₂O₂ for 30 min at room temperature to block endogenous peroxidase activity, and then incubated in the TUNEL reaction mixture for 60 min at 37 °C, and visualized by fluorescence microscopy (DM4000B; Leica Wetzlar, Germany).

Western blot analysis

Briefly, the proteins were electrophoresed by sodium dodecyl sulfate polyacrylamide gel (Bio-Rad) and transferred to polyvinylidene fluoride membranes (Millipore, MA). The membranes were blocked with 5 % skimmed milk in tris-buffered saline-Tween (TBST) and then incubated with a primary antibody with gentle shake at 4 °C for 12 h. Further, the membranes were washed three times with TBST and incubated with a peroxidase-conjugated secondary antibody. Primary antibodies including anti-MEF2D, anti-Ki67, anti- β -catenin and anti-phosphorylated β -catenin antibodies (Abcam, Cambridge, UK), and anti-cleaved caspase-3 (Sigma, St. Louis, MO, USA) were used. GAPDH (Sigma, St. Louis, MO, USA) was used as an internal control. The target protein was visualized by an enhanced chemiluminescence (ECL) detection system (Invitrogen-Life Technologies, Carlsbad, CA, USA). All values were calculated as ratios normalized to GAPDH.

Tumorigenesis assay

AGS cells (5×10^7) infected with Lv-scramble or Lv-shMEF2D (MOI=10) (Shanghai Genepharma Co. Ltd., Shanghai, China) diluted in 200 μ L PBS were injected subcutaneously into the right groin of BALB/c nude mice. The tumor volume was measured daily, and the tumor was removed at the 35 days post-inoculation. The length and width were measured, and the volume was calculated using the formula: length \times width² \times $\pi/6$.

miR-19 inhibitor and mimics

mirVanaTM miRNA inhibitors (30 nM) or mimics (30 nM) for miR-19 or control molecules (30 nM) (Invitrogen, Carlsbad, CA) with LipofectamineTM 2000 was transfected into the indicated cells, 48 h prior to subsequent experiments.

Dual-luciferase reporter assay

The MEF2D 3'-UTR and mutated 3'-UTR constructs were amplified and sub-cloned into pGL3 Luciferase Promote Vector (Sangon, Shanghai, China) with XbaI and NotI restriction sites. Using Lipofectamine transfection reagent (Sangon, Shanghai, China), the pGL3 vector containing MEF2D 3'-UTR or mutated forms was co-transfected with or without miR-19 mimics (Invitrogen, Carlsbad, CA) into AGS cells according to the manufacturer's instruction. The cells were collected after 48-h transfection, and the luciferase activity was measured using the Dual-Luciferase Reporter Assay Kit (Sangon, Shanghai, China).

TOPflash luciferase reporter assay

Cells infected with lentivirus for shMEF2D, or lentivirus-scramble were plated in 24-well plates, at a density of 2×10^5 cells in 500 μ L media per well. The co-transfection solution (100 μ L per well) was made by mixing 750 ng of TOPflash reporter plasmid or 750 ng of FOPflash reporter plasmid with 50 ng TK-Renilla plasmid (for a total of 800 ng) and 2 μ L of Lipofectamine 2000 Transfection Reagent (Invitrogen, Carlsbad, CA). The transfection mixture was incubated at room temperature for 15 min. Meanwhile, the growth media were removed from each well, and 400 μ L of serum-free DMEM was added before the 100 μ L transfection mixture was added. Seventy-two hours later, the cells were lysed in passive lysis buffer (Promega, Madison, WI) and luciferase activities were measured using the Dual-Luciferase Assay System (Promega, Madison, WI) and a Veritas Microplate Luminometer (Turner Biosystems, Promega, Madison, WI). Firefly luciferase activity was normalized to activity of Renilla luciferase.

Statistical analysis

Data were presented as mean \pm SD from at least three independent experiments. Data between categorical variables were analyzed by the χ^2 and Fisher's exact tests. Survival analysis was performed by Kaplan-Meier plot and log-rank tests. Multivariate analysis was based on the Cox proportional hazards regression model. Data between or among groups were analyzed by two-tailed Student's *t* test or one-way ANOVA by SPSS 19.0 software (SPSS Inc., Chicago, IL, USA), respectively. $p < 0.05$ was considered to be statistically significant.

Results

MEF2D was increased in gastric cancer

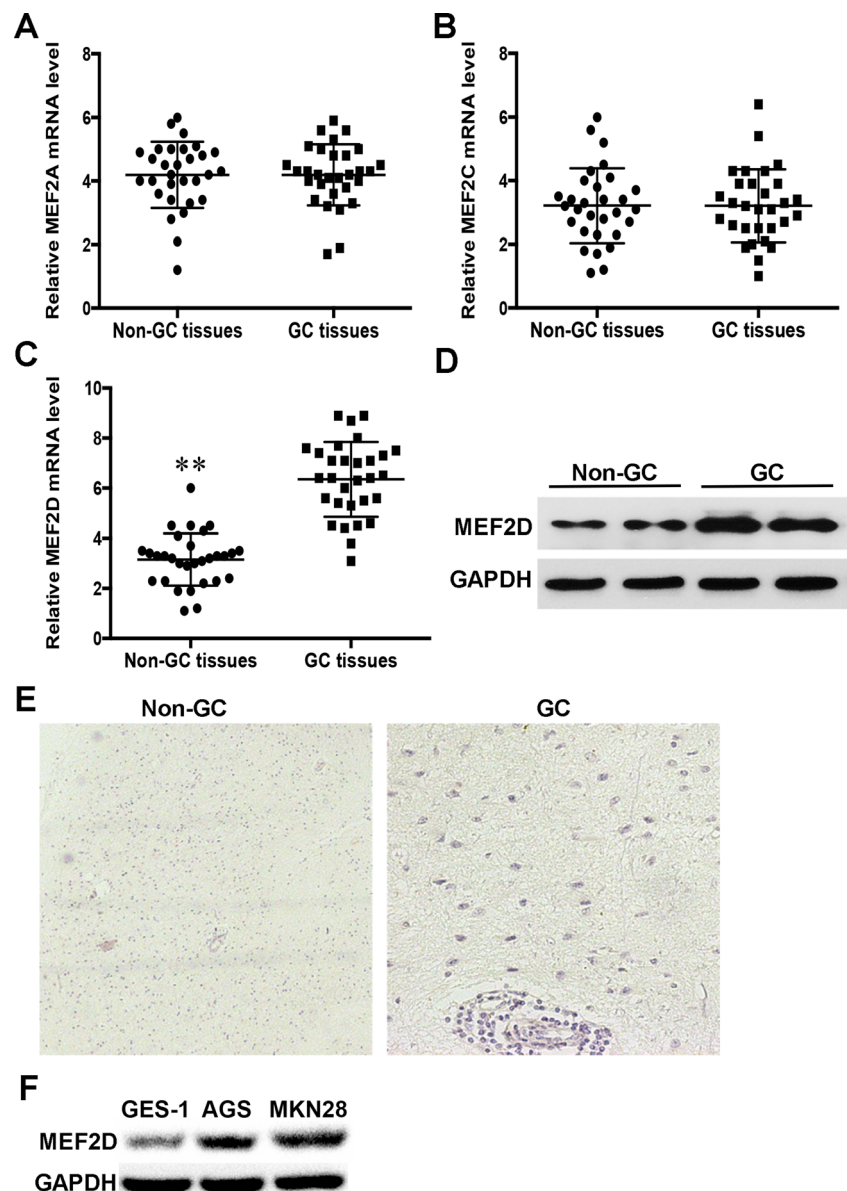
To investigate the expression profile of MEF2s in GC specimens, we applied qPCR to measure mRNA level of MEF2A, 2B, 2C, and 2D in 30 fresh gastric cancer samples and their corresponding non-GC tissues. Results showed that there were no significant differences in MEF2A and MEF2C mRNA between GC and non-GC tissues (Fig. 1a, b). There is no detectable MEF2B mRNA in these tissues (data not shown). However, the abundance of MEF2D mRNA was significantly increased in GC than non-GC tissues (Fig. 1c). Further, we determined MEF2D expression in GC tissues at protein level

by western blot and immunohistochemistry. Compared with the non-GC tissues, MEF2D protein level was markedly elevated in GC samples (Fig. 1d, e). Finally, we detect the levels of MEF2D in GC cell lines. Our results showed that, compared with normal human gastric epithelial cell line (GES-1), the levels of MEF2D in GC cell lines (AGS and MKN28) were obviously increased (Fig. 1f).

Immunohistochemical analysis of MEF2D expression and the association with clinicopathological parameters

To explore the clinicopathological significance of MEF2D, we performed immunohistochemical analysis in 260 paraffin-embedded gastric cancer tissues. The results were

Fig. 1 MEF2D was increased in gastric cancer. **a, b, c** MEF2A, MEF2C, and MEF2D mRNA levels were determined by qPCR in the collected gastric cancer (GC) specimen and the corresponding normal (non-GC) tissues ($n=8$). Data were presented as mean \pm SD. ****** $p < 0.01$ compared with the non-GC tissues. **d** Western blot was used to evaluate MEF2D protein level in GC tissues and the matched normal tissues (non-GC). GAPDH was used as loading control. **e** Immunohistochemistry was applied to detect MEF2D in GC tissues and the matched normal tissues (non-GC). **f** Western blot analysis of MEF2D expression levels in GC cell lines (AGS and MKN28 cells) compared with normal human gastric epithelial cell line (GES-1 cells)



classified for the MEF2D expression as negative for MEF2D expression or positive for MEF2D expression based on the scores. As shown in Fig. 2, scores of 0 or 1+ were considered to indicate a lack of MEF2D expression, and scores of 2+ or 3+ were considered to indicate the presence of MEF2D expression. The expression rate of MEF2D in GC tissues was 70.4 % (183/260); however, the expression rate in paired adjacent non-GC samples was only 9.6 % (25/260). The association between MEF2D expression and several clinicopathological parameters was shown in Table 1. The results suggested that MEF2D expression was closely related with the clinical stage of GC, incidence of vascular invasion, metastasis, and tumor size.

Association between MEF2D expression and prognosis

The prognostic effect of MEF2D expression in patients with GC was analyzed. The results revealed that the overall survival duration of the patients with MEF2D expression was significantly shorter as compared with that of the patients lacking of MEF2D expression (Fig. 3). Furthermore, multivariate analysis demonstrated that the overall survival time of patients was significantly associated with MEF2D presence (Table 2). Also, the multivariate analysis showed metastasis and vascular invasion to be independent prognostic factors.

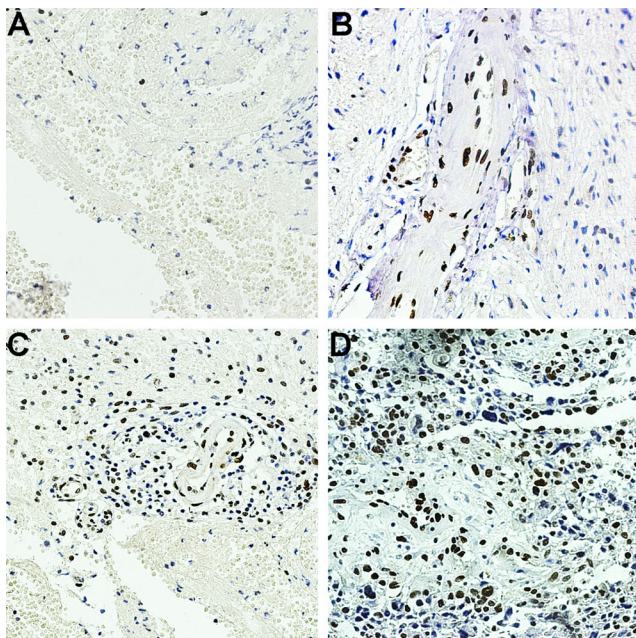


Fig. 2 Representative samples of the immunohistochemical scoring of gastric cancer tissues. MEF2D expression was analyzed with immunohistochemistry in gastric cancer tissues. We scored the results of immunohistochemistry using the 0 to 3+ scale. Scores of **a** 0 or **b** 1+ were considered to be negative for MEF2D expression, and **c** 2+ and **d** 3+ were considered to be positive for MEF2D expression

Table 1 Association between MEF2D expression and clinicopathological parameters in 260 patients with gastric cancer

Parameters	Total, <i>n</i>	MEF2D expression		<i>p</i> Value
		Present, <i>n</i>	Absent, <i>n</i>	
Total	260	183	77	
Age				NS
<48	102	62	40	
>48	158	95	63	
Gender				NS
Male	160	103	57	
Female	100	71	29	
Clinical stage				<0.05
I–II	73	38	35	
III–IV	187	156	31	
T-stage				NS
T1–T2	84	63	21	
T3–T4	176	134	42	
N-stage				NS
N0	92	49	43	
N1–N3	168	88	80	
Vascular invasion				<0.05
No	192	36	156	
Yes	68	45	23	
Metastasis				<0.05
No	195	116	79	
Yes	65	54	11	
Tumor size				<0.05
<5 cm	102	36	66	
>5 cm	158	99	59	

NS not significant, *T-stage* tumor stage, *N-stage* stage of lymph node involvement

MEF2D silencing depressed the growth and survival of GC cells

To explore the function of MEF2D in GC cells, we constructed a lentiviral vector carrying shRNA that specifically knocked down MEF2D expression (Lv-shMEF2D). Data confirmed that Lv-shMEF2D specifically decreased MEF2D level in AGS and MKN28 GC cell lines (Fig. 4a). Lv-shMEF2D significantly suppressed the proliferation rates of AGS and MKN28 cells, compared with Lv-scramble (Fig. 4b, c). In addition, western blot showed that Lv-shMEF2D induced cleaved caspase3 upregulation and Ki67 downregulation (Fig. 4d). Finally, TUNEL assay indicated that Lv-shMEF2D elevated apoptotic death in both cell lines (Fig. 4e). Taken together, the above results suggested that MEF2D inhibition reduced the proliferation and survival of GC cells.

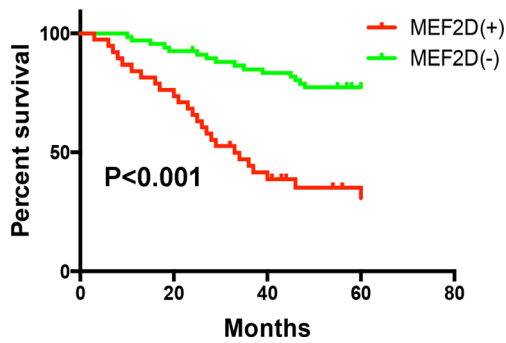


Fig. 3 Kaplan-Meier survival curves of 260 patients with gastric cancer subject to gastrectomy. The overall survival time of patients with MEF2D expression was significantly shorter than that of patients negative for MEF2D expression ($p < 0.001$)

MEF2D suppression inhibited the activation of Wnt/ β -catenin pathway

Emerging evidence indicate that Wnt/ β -catenin is an oncogenic pathway involved in gastric carcinogenesis [19–21]. Thus, we applied western blot and luciferase assay to explore the potential effect of MEF2D suppression on Wnt/ β -catenin pathway. Results revealed that MEF2D downregulation via Lv-shMEF2D significantly inhibited the activation of Wnt/ β -catenin pathway in both AGS and MKN28 GC cells, as indicated by increased level of phosphorylated β -catenin and lower level of β -catenin (Fig. 5a, c) and decreased luciferase expression of TOPflash reporter (Fig. 5b, d). Our data suggested that MEF2D reduction inactivated Wnt/ β -catenin pathway.

Table 2 Multivariate analysis of the prognosis in patients with gastric cancer

Variables	HR (95 % CI)	<i>p</i> Value
Depth of invasion		
T1 + T2 vs. T3 + T4	0.842 (0.124–2.317)	0.087
Nodal status		
N0 vs. N1 + N2 + N3	1.038 (0.233–2.985)	0.092
Metastasis		
Absent vs. present	8.721 (3.427–18.563)	<0.001
Stage		
I + II vs. III + IV	0.914 (0.289–2.341)	0.082
Vascular invasion		
Absent vs. present	2.183 (1.001–3.491)	0.024
MEF2D		
Absent vs. present	2.962 (1.985–6.449)	0.013

HR hazard ratio, CI confidence interval

MEF2D reduction suppressed tumorigenesis of gastric cancer cells

The role of MEF2D in tumor formation of GC cells was also investigated in BALB/c nude mice. Lv-shMEF2D- or Lv-scramble-infected AGS cells were subcutaneously injected in nude mice, and 35 days later, tumors were removed. Results showed that Lv-shMEF2D-infected AGS cells formed tumors much smaller than that in Lv-scramble-infected AGS cells (Fig. 6a). The average weight and volume of tumors were significantly lower in Lv-shMEF2D-infected groups than that in the Lv-scrambled-infected groups (Fig. 6b, c). Western blot analysis revealed extensive expression of MEF2D in tumors from the Lv-scrambled-infected group, whereas MEF2D expression was not detectable in the formed tumors from Lv-shMEF2D-infected groups (Fig. 6d). These data showed that MEF2D reduction blocked gastric cancer formation in vivo.

miR-19 reduced the expression of MEF2D and activation of Wnt/ β -catenin signaling

We used TargetScan on the internet to explore the possible microRNA that regulates MEF2D. Luckily, we found that MEF2D was one of the potential targets of miR-19. The predicted binding of miR-19 with MEF2D 3'-UTR was illustrated (Fig. 7a). miR-19 inhibitor increased MEF2D expression in GC cells (Fig. 7b, c), while miR-19 mimic was capable to reduce MEF2D level (Fig. 7d, e). To further validate interaction between miR-19 and MEF2D, the MEF2D complementary sites, with or without mutations, were cloned into the 3'-UTR of the firefly luciferase gene and co-transfected with miR-19 mimics in AGS cells. Our results showed that the presence of miR-19 led to a significant reduction in the relative luciferase activity of the wild-type construct of MEF2D 3'-UTR in AGS cells. However, the mutant (MUT) construct of MEF2D 3'-UTR abolished such the suppressive effect of miR-19 in AGS cells (Fig. 7f). The above results demonstrated that MEF2D is the direct target of miR-19. Furthermore, miR-19 was significantly reduced in the collected gastric cancer specimens (Fig. 8a).

Finally, we explored whether miR-19 affected Wnt/ β -catenin pathway with western blot. Results showed that miR-19 inhibitor significantly activated while miR-19 mimics inactivated Wnt/ β -catenin pathway (Fig. 8b–d).

Discussion

In the present study, we found that only MEF2D rather than MEF2A, 2B, or 2C was elevated in gastric cancer

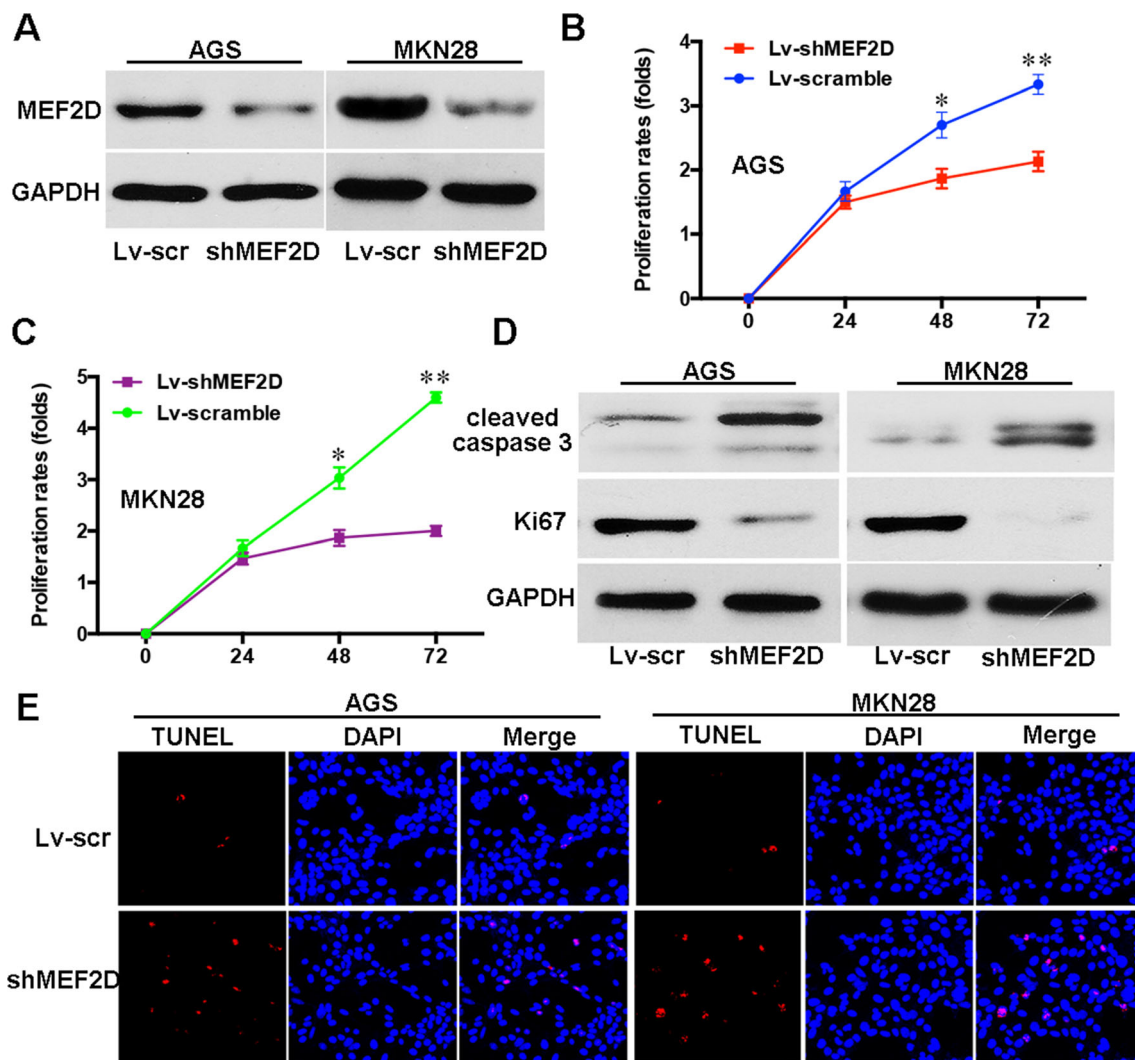


Fig. 4 MEF2D silencing depressed the growth of GC cells. **a** MEF2D level was detected via western blot in two gastric cell lines (AGS and MKN28 cells) at 72 h after infection with Lv-scramble (Lv-scr) and Lv-shMEF2D at MOI of 10. GAPDH was used as loading control. **b**, **c** The proliferation rates of AGS and MKN28 cells in which MEF2D expression was reduced via lentivirus were determined. Data were presented as mean \pm SD from three independent experiments. * $p < 0.05$ and

** $p < 0.01$ compared with the Lv-scramble groups. **d** Cleaved caspase 3 and Ki67 were assessed with western blot in AGS and MKN28 cells at 72 h after infection with Lv-scramble (Lv-scr) and Lv-shMEF2D at MOI of 10. GAPDH was used as loading control. **e** TUNEL assay was conducted to detect the apoptosis in AGS and MKN28 cells after MEF2D was suppressed. Red, apoptotic cells. Blue, nuclear

clinical specimens. Furthermore, immunohistochemical analysis on the tissue samples obtained from 260 patients with gastric cancer revealed that MEF2D expression was significantly associated with the clinical stage, vascular invasion, metastasis, and tumor size. Gastric cancer patients with MEF2D expression showed a significantly shorter overall survival time compared with that of patients lacking of MEF2D. Multivariate analysis revealed that MEF2D expression was an independent prognostic factor for overall survival. These results indicated that MEF2D was a prognostic marker for gastric cancer. Importantly, downregulation of MEF2D via Lv-shMEF2D was able to reduce the proliferation and

survival of gastric cancer cells. Further study revealed that MEF2D suppression significantly inactivated the oncogenic Wnt/ β -catenin pathway. Downregulation of MEF2D inhibited the tumorigenesis of gastric cancer cells in nude mice. Finally, we found that miR-9 directly targeted MEF2D and markedly inhibited activation of Wnt/ β -catenin pathway. Moreover, we confirmed the reverse relationship between miR-9 and MEF2D in the collected clinical gastric cancer specimens.

Previous studies reveal that MEF2C and MEF2D function as oncogenes in T cell acute lymphoblastic leukemia and chronic myeloid leukemia [16, 22–25]. MEF2D is upregulated in nasopharyngeal carcinoma

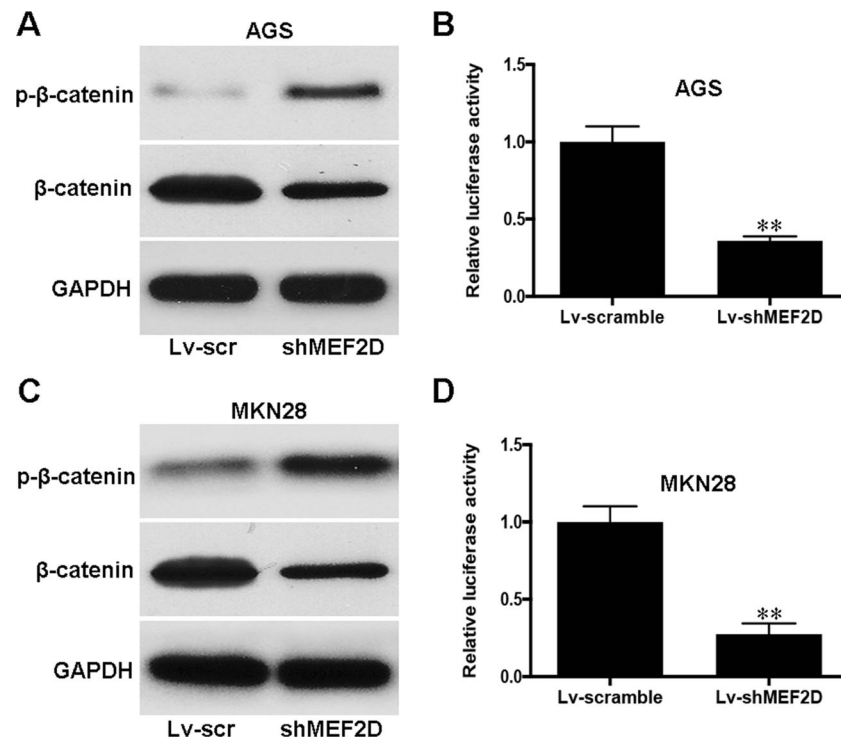


Fig. 5 MEF2D suppression inhibited the activation of Wnt/β-catenin pathway. **a** AGS cells were infected with Lv-scramble (Lv-scr) and Lv-shMEF2D at MOI of 10 for 72 h, followed by western blot for phosphorylated (p-β-catenin) and total β-catenin level. GAPDH was used as loading control. **b** When Lv-scramble or Lv-shMEF2D was added, TOPflash reporter plasmids were transfected into AGS cells together with pRL-TK plasmid. Seventy-two hours later, luciferase

activity was quantified to detect the activation of Wnt signaling pathway. **c, d** MKN28 cells were treated as above. Western blot was used to evaluate the level of phosphorylated (p-β-catenin) and total β-catenin level. Luciferase level was also quantified to detect the Wnt signaling activity. Data were presented as mean ± SD from three independent experiments. ** $p < 0.01$ compared with the Lv-scramble groups

tissues [26]. MEF2B mutations lead to deregulated expression of the oncogene BCL6 in diffuse large B cell

lymphoma [27–29]. Dysregulation of MEF2D inhibits differentiation and contributes to oncogenesis in

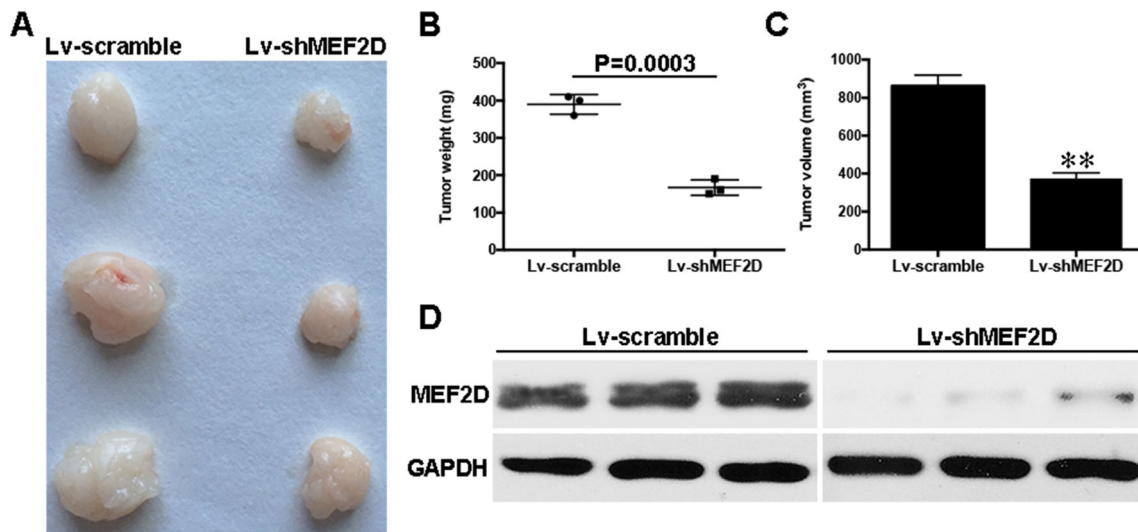


Fig. 6 MEF2D reduction suppressed tumorigenesis of gastric cancer cells. **a** AGS cells infected with Lv-scramble or Lv-shMEF2D (MOI=10) were subcutaneously inoculated into BALB/c nude mice. Thirty-five days later, tumors were removed. **b, c** The weight and volume of formed tumors were measured. **d** Western blot analysis of

MEF2D level was performed in AGS tumor xenografts. GAPDH was used as loading control. Data were presented as mean ± SD from three independent experiments. ** $p < 0.01$ compared with the Lv-scramble groups

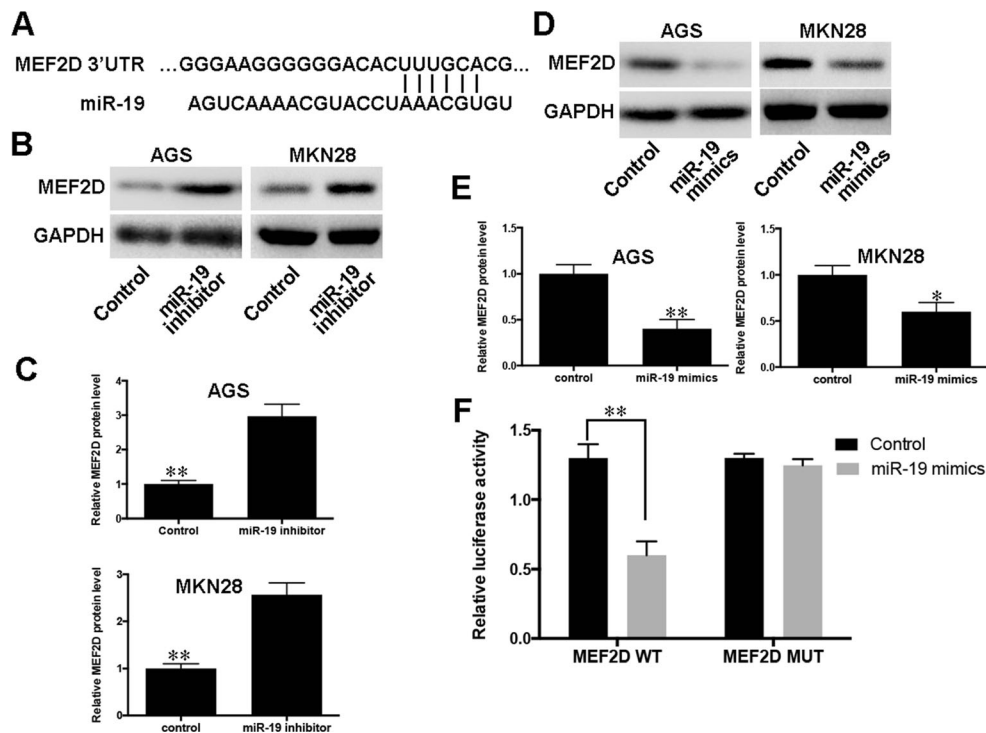


Fig. 7 miR-19 directly targeted MEF2D and decreased its expression. **a** A potential miR-19 recognition site (MRE) is located in the 3'-UTR of MEF2D mRNA. **b, c** AGS and MKN28 cells were transduced with miR-19 inhibitor (50 nM) for 24 h and followed by western blot analysis of MEF2D protein expression. GAPDH was used as loading control. Band density was measured with Image J (version 7.0), and data were presented as mean \pm SD from three independent experiments. $**p < 0.01$ compared with the control groups. **d, e** AGS and MKN28 cells were transduced with miR-19 mimics (50 nM) for 24 h and followed by western blot analysis of MEF2D protein expression. GAPDH was used as loading control. Band density was measured with Image J (version 7.0), and data were presented

as mean \pm SD from three independent experiments. $*p < 0.05$ and $**p < 0.01$ compared with the control groups. **f** The interaction between miR-19 and MEF2D was determined by luciferase activity assays. The wild-type or mutant MEF2D 3'-UTR was co-transfected with miR-19 mimics or scramble miRNA (control) and incubated for 48 h into AGS cells followed with a detection by dual-luciferase reporter assay kit. *wt* denotes pGL3 vectors containing MEF2D 3'-UTR; *mut* denotes pGL3 vectors containing mutated MEF2D 3'-UTR. Data were presented as mean \pm SD from three independent experiments. $**p < 0.01$ compared with the indicated group

rhabdomyosarcoma cells [30]. In addition, studies confirm that MEF2D promotes tumorigenesis in lung carcinoma [17, 18]. Further, MEF2s promote EMT through TGF- β 1 auto regulation circuitry [14]. However, study about the expression profile and the potential role of MEF2 family members in gastric cancer is still lacking. Data from our study provides, for the first time, that only MEF2D rather than other family members is increased in clinical gastric cancer specimens. Importantly, reducing MEF2D via lentivirus inhibits the proliferation and survival of gastric cancer cells. These data favor an oncogenic role of MEF2D in gastric cancer.

Wnt/ β -catenin pathway has been cell established to play an oncogenic role in many cancers. Recent studies demonstrate that ZNRF3 contributes to the growth of lung carcinoma via inhibiting Wnt/ β -catenin pathway and is regulated by miR-93 [31]. Inhibition of oleandrin on the proliferation and invasion of osteosarcoma cells in vitro by suppressing Wnt/ β -catenin signaling pathway [32]. IWR-1 inhibits epithelial-

mesenchymal transition of colorectal cancer cells through suppressing Wnt/ β -catenin signaling as well as survivin expression [33]. MAGI3 negatively regulates Wnt/ β -catenin signaling and suppresses malignant phenotypes of glioma cells [34]. In the present study, for the first time, our results demonstrate that MEF2D silencing significantly inactivates Wnt/ β -catenin pathway. Further studies are needed to explore the underlying mechanism of MEF2D inhibition on Wnt/ β -catenin signaling.

Finally, to explore the possible regulatory mechanism of MEF2D upregulation in gastric cancer, we used online database to identify the possible miRNAs involved in regulating MEF2D. The data suggested that miR-19 might be a miRNA that can suppress MEF2D expression. This finding was further confirmed by experimental approaches. Further, our data confirm that miR-19 is significantly decreased in clinical gastric cancer specimens. Interestingly, our present study demonstrates that miR-19 is able to suppress Wnt/ β -catenin pathway.

In conclusions, our study demonstrates that miR-19/MEF2D/Wnt/ β -catenin regulatory network contributes to

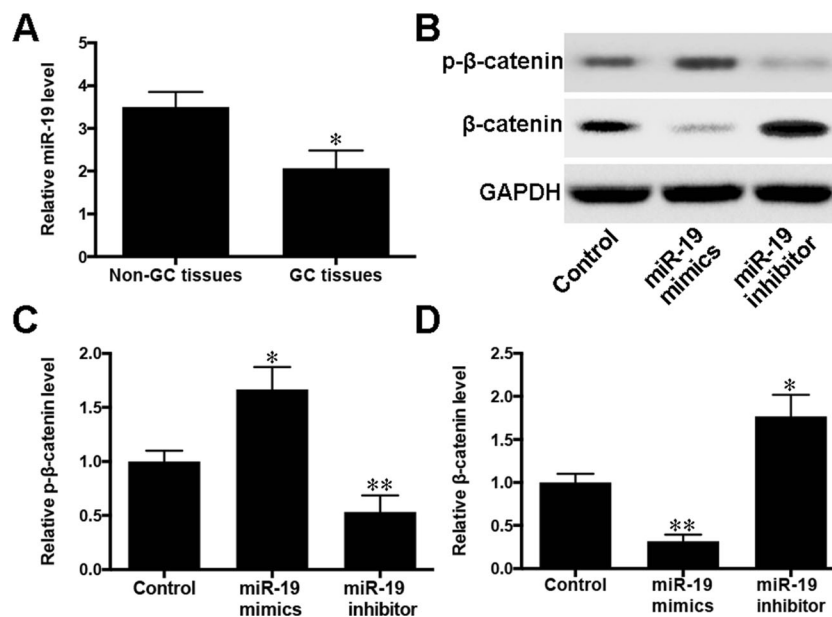


Fig. 8 miR-19 was decreased in gastric cancer and affected Wnt/ β -catenin signaling. **a** miR-19 levels were determined by qPCR in the collected gastric cancer (GC) specimen and the corresponding normal (non-GC) tissues ($n=8$). Data were presented as mean \pm SD. $*p < 0.05$ compared with the non-GC tissues. **b** AGS cells were transduced with miR-19 mimics or miR-19 inhibitor (50 nM) for 24 h and followed by

western blot analysis of phosphorylated (p- β -catenin) and total β -catenin level. GAPDH was used as loading control. **c**, **d** Density of bands in (b) were determined with Image J (version 7.0). Data were presented as mean \pm SD from three independent experiments. $*p < 0.05$ and $**p < 0.01$ compared with the control group

the growth of gastric cancer, providing a novel molecular target for future gastric cancer therapy.

Acknowledgments The authors thank Prof. Li from the Center of Cancer Research, Boston University, USA, for the critical reading and modification of the manuscript.

Compliance with ethical standards

Conflicts of interest None

References

- Shah MA, Kelsen DP. Gastric cancer: a primer on the epidemiology and biology of the disease and an overview of the medical management of advanced disease. *J Natl Compr Cancer Netw*. 2010;8:437–47.
- Compare D, Rocco A, Nardone G. Risk factors in gastric cancer. *Eur Rev Med Pharmacol Sci*. 2010;14:302–8.
- Lynch HT, Grady W, Suriano G, Huntsman D. Gastric cancer: new genetic developments. *J Surg Oncol*. 2005;90:114–33.
- Aung P, Oue N, Mitani Y, Nakayama H, Yoshida K, Noguchi T, et al. Systematic search for gastric cancer-specific genes based on sage data: melanoma inhibitory activity and matrix metalloproteinase-10 are novel prognostic factors in patients with gastric cancer. *Oncogene*. 2006;25:2546–57.
- Sun W, Wu Y, Yu X, Liu Y, Song H, Xia T, et al. Decreased expression of long noncoding rna ac096655. 1–002 in gastric cancer and its clinical significance. *Tumor Biol*. 2013;34:2697–701.
- Sakakura C, Hagiwara A, Miyagawa K, Nakashima S, Yoshikawa T, Kin S, et al. Frequent downregulation of the runt domain transcription factors runx1, runx3 and their cofactor cbfb in gastric cancer. *Int J Cancer*. 2005;113:221–8.
- Li Q, Zhang N, Jia Z, Le X, Dai B, Wei D, et al. Critical role and regulation of transcription factor foxm1 in human gastric cancer angiogenesis and progression. *Cancer Res*. 2009;69:3501–9.
- Li T, Lu Y, Zhao X, Guo H, Liu C, Li H, et al. MicroRNA-296-5p increases proliferation in gastric cancer through repression of caudal-related homeobox 1. *Oncogene*. 2014;33:783–93.
- Wang B, Cai Z, Lu F, Li C, Zhu X, Su L, et al. Destabilization of survival factor mef2d mRNA by neurotoxin in models of Parkinson's disease. *J Neurochem*. 2014;130:720–8.
- Black BL, Olson EN. Transcriptional control of muscle development by myocyte enhancer factor-2 (mef2) proteins. *Annu Rev Cell Dev Bi*. 1998;14:167–96.
- Bai X, Wu L, Liang T, Liu Z, Li J, Li D, et al. Overexpression of myocyte enhancer factor 2 and histone hyperacetylation in hepatocellular carcinoma. *J Cancer Res Clin*. 2008;134:83–91.
- Bai X, Zhang Q, Ye L, Liang F, Sun X, Chen Y, et al. Myocyte enhancer factor 2c regulation of hepatocellular carcinoma via vascular endothelial growth factor and wnt/ β -catenin signaling. *Oncogene*. 2014.
- Ma L, Liu J, Liu L, Duan G, Wang Q, Xu Y, et al. Overexpression of the transcription factor mef2d in hepatocellular carcinoma sustains malignant character by suppressing g2–m transition genes. *Cancer Res*. 2014;74:1452–62.
- Yu W, Huang C, Wang Q, Huang T, Ding Y, Ma C, et al. Mef2 transcription factors promotes emt and invasiveness of hepatocellular carcinoma through tgf- β 1 autoregulation circuitry. *Tumor Biol*. 2014;35:10943–51.
- Shin H-M, Seoh J-Y, Chung H-Y, Choi S-J, Hahn M-J, Kang J-S, et al. Requirement of mef2d in the induced differentiation of h160 promyeloid cells. *Mol Immunol*. 1999;36:1209–14.
- Prima V, Gore L, Caires A, Boomer T, Yoshinari M, Imaizumi M, et al. Cloning and functional characterization of mef2d/dazap1 and dazap1/mef2d fusion proteins created by a variant t (1; 19)(q23;

- p13. 3) in acute lymphoblastic leukemia. *Leukemia*. 2005;19:806–13.
17. Zhao X, Liu M, Li D. Oleonic acid suppresses the proliferation of lung carcinoma cells by mir-122/cyclin g1/mef2d axis. *Mol Cell Biochem*. 2015;400:1–7.
 18. Song L, Li D, Zhao Y, Gu Y, Zhao D, Li X, et al. Mir-218 suppressed the growth of lung carcinoma by reducing mef2d expression. *Tumor Biol*. 2015;1–10.
 19. Zhang H, Xue Y. Wnt pathway is involved in advanced gastric carcinoma. *Hepato-gastroenterol*. 2007;55:1126–30.
 20. Cai C, Zhu X. The wnt/ β -catenin pathway regulates self-renewal of cancer stem-like cells in human gastric cancer. *Molecular medicine reports*. 2012;5:1191–6.
 21. Huang J, Xiao D, Li G, Ma J, Chen P, Yuan W, et al. Epha2 promotes epithelial–mesenchymal transition through the wnt/ β -catenin pathway in gastric cancer cells. *Oncogene*. 2014;33:2737–47.
 22. Homminga I, Pieters R, Langerak AW, de Rooi JJ, Stubbs A, Verstegen M, et al. Integrated transcript and genome analyses reveal nkx2-1 and mef2c as potential oncogenes in t cell acute lymphoblastic leukemia. *Cancer Cell*. 2011;19:484–97.
 23. Nagel S, Meyer C, Quentmeier H, Kaufmann M, Drexler H, MacLeod R. Mef2c is activated by multiple mechanisms in a subset of t-acute lymphoblastic leukemia cell lines. *Leukemia*. 2008;22:600–7.
 24. Lilljebjörn H, Ågerstam H, Orsmark Pietras C, Rissler M, Ehrencrona H, Nilsson L, et al. Rna-seq identifies clinically relevant fusion genes in leukemia including a novel mef2d/csfl1r fusion responsive to imatinib. *Leukemia*. 2014;28:977–9.
 25. Schwieger M, Schüler A, Forster M, Engelmann A, Arnold MA, Delwel R, et al. Homing and invasiveness of mll/enl leukemic cells is regulated by mef2c. *Blood*. 2009;114:2476–88.
 26. Li Y, Zhang L, Nong J, Bian S, Zhao Z, Ren Y, et al. Expression of mef2d on nasopharyngeal carcinoma tissues and its influence of prognostic. *Lin chuang er bi yan hou tou jing wai ke za zhi* = Journal of clinical otorhinolaryngology, head, and neck surgery. 2011;25:840–2. 847.
 27. Lohr JG, Stojanov P, Lawrence MS, Auclair D, Chapuy B, Sougnez C, et al. Discovery and prioritization of somatic mutations in diffuse large b-cell lymphoma (dlbcl) by whole-exome sequencing. *Proc Natl Acad Sci*. 2012;109:3879–84.
 28. Tagawa H, Suguro M, Tsuzuki S, Matsuo K, Karnan S, Ohshima K, et al. Comparison of genome profiles for identification of distinct subgroups of diffuse large b-cell lymphoma. *Blood*. 2005;106:1770–7.
 29. Zhang J, Grubor V, Love CL, Banerjee A, Richards KL, Mieczkowski PA, et al. Genetic heterogeneity of diffuse large b-cell lymphoma. *Proc Natl Acad Sci*. 2013;110:1398–403.
 30. Zhang M, Truscott J, Davie J. Loss of mef2d expression inhibits differentiation and contributes to oncogenesis in rhabdomyosarcoma cells. *Mol Cancer*. 2013;12:1–14.
 31. Shi J, Jiang X, Yu Z, He G, Ning H, Wu Z, et al. Znf3 contributes to the growth of lung carcinoma via inhibiting wnt/ β -catenin pathway and is regulated by mir-93. *Tumor Biol*. 2015;1–7.
 32. Ma Y, Zhu B, Liu X, Yu H, Yong L, Liu X, et al. Inhibition of oleandrin on the proliferation and invasion of osteosarcoma cells in vitro by suppressing wnt/ β -catenin signaling pathway. *J Exp Clin Canc Res*. 2015;34:1.
 33. Lee SC, Kim O-H, Lee SK, Kim S-J. Iwr-1 inhibits epithelial-mesenchymal transition of colorectal cancer cells through suppressing wnt/ β -catenin signaling as well as survivin expression. *Oncotarget*. 2015;6:27146–59.
 34. Ma Q, Yang Y, Feng D, Zheng S, Meng R, Fa P, et al. Magi3 negatively regulates wnt/ β -catenin signaling and suppresses malignant phenotypes of glioma cells. *Oncotarget*. 2015.